Spectrophotometric Determination and Computational Evaluation of the Rates of Hydrolysis of 9-Amino-Substituted Acridines

John R. Goodell, Bengt Svensson, and David M. Ferguson*

Department of Medicinal Chemistry and Center for Drug Design, University of Minnesota Supercomputer Institute, University of Minnesota, Minneapolis, Minnesota 55455

Received August 11, 2005

Aminoacridines have a long history in the drug and dye industries and display a wide range of biological and physical properties. Despite the historical relevance of 9-aminoacridines, there have been few studies investigating their stability. 9-Aminoacridines are known to hydrolyze at the C^9-N^{15} bond, yielding acridones. In this study, the pH-dependent hydrolysis rates of a series of 9-substituted aminoacridines are investigated. In addition, ground-state physical properties of the compounds are determined using ab initio quantum mechanics calculations to gain insight into the forces that drive hydrolysis. An analysis of the bond orders, bond dissociation energies, and conformational energies show that the rate of hydrolysis depends on two main factors: delocalization across the C^9-N^{15} bond and steric effects. The computational results are applied to explain the change in experimental rates of hydrolysis going from primary to secondary and to tertiary substituted 9-aminoacridines. In the case of tertiary substituted amines, the calculations indicate the C^9-N^{15} bond is forced into a more gauche-like conformation, greatly diminishing delocalization (as shown by reductions in bond orders and bond energy), which leads to rapid hydrolysis. A model of intramolecular hydrogen bonding is also presented, which explains the increased rate of hydrolysis observed for highly substituted compounds under acidic conditions.

INTRODUCTION

Aminoacridines are the most important and attractive class of all acridines. In addition, they represent the majority of acridine drugs and dyes.[1−4] Aminoacridines also display a wide range of biological and physical properties. Among all the monoamine isomers, 9-aminoacridines have the most significant history in the drug industry.[1,3] The antibacterial activity of 9-aminoacridine (**1**) was long overlooked and not utilized until the Second World War. Quinacrine (**2**) is arguably the best known 9-amino-containing acridine drug. It was commonly used as an antimalarial until recently, as resistant strains of malaria have emerged.[1−3] Most recently, amsacrine (**3**) was developed with the intended use as an anticarcinogenic agent.[4] Compound **1** shows the numbering scheme for the acridine core scaffold.

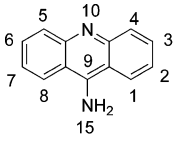

(1)

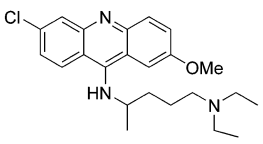

(2)

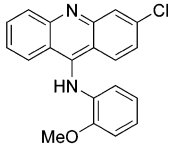

(3)

Recent work in our laboratory investigating the use of 9-aminoacridines as broad spectrum antivirals has prompted an in-depth examination of the stability of compounds bearing aminoalkyl substitutions. This study aims to aid in the design and selection of the next generation of 9-amino-acridine drugs for biological targets.

* Corresponding author phone: (612) 626-2601; fax: (612) 626-4429; e-mail: ferguson@umn.edu.

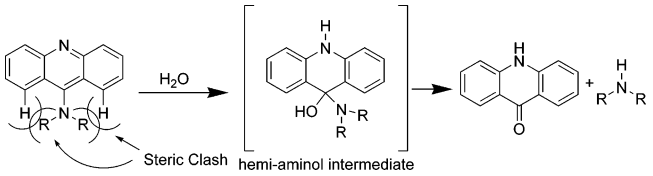

Figure 1. Steric clashes and reaction path.

The stability of 9-aminoacridines has received little investigation despite the historical relevance of acridine drugs containing 9-amino substitutions. However, the discussion of 9-aminoalkylacridine stability is not a new one by any means. It has long been proposed that an increase of steric bulk around the 9-amino produces steric interactions which result in a weakening of the C^9-N^{15} bond.[1] Thus, the rate of hydrolysis to the acridone and the amine increases with the amount of steric bulk. The hydrolysis reaction is depicted in Figure 1. Understanding the stability of 9-aminoacridines requires understanding the resonating nature of these unique bases. Amino substitutions at the C^9 position of acridine are intriguing because of the resonance of the exocyclic nitrogen into the aromatic ring, resulting in an increase in base strength. For example, the pK_a for acridine is around 5, while the pK_a for 9-aminoacridine is around 10.[1] Amino compounds of this sort are often referred to as vinylogous amidines having two nitrogens separated by one or more double bonds. Because of the resonating nature of 9-aminoacridines, the exocyclic nitrogen is coplanar with the tricycle. This is observed both under protonated and nonprotonated conditions. However, the effect is much more prominent when the molecule is protonated. Spectrophotometric investigation of 9-aminoacridine has shown that protonation occurs at the

10.1021/ci050322s CCC: $33.50
Published on Web 01/06/2006

nitrogen in the acridine ring rather than the exocyclic nitrogen and that a second protonation does not occur.[1]

Studies on the rate of hydrolysis for 9-aminoacridines have been limited. Ledóchowski and co-workers conducted a series of hydrolysis reactions on 9-aminoacridine, 9-methylaminoacrindine, and 9-(3-dimethyl(aminopropyl)amino)-acridine.[5] They concluded that hydrolysis is favored under alkaline conditions, lending to the hypothesis that hydrolysis occurs via nucleophilic displacement by the hydroxide ion. However, they did not elaborate on the effect of alkyl substitution on the hydrolysis rate. The authors stated that steric hindrance may influence hydrolysis by bending the C^9-N^{15} bond away from coplanarity, making the approach of the nucleophilic hydroxide ion difficult. Conversely, they remark that nucleophilic attack is more favorable at the C^9 position when the acridine molecule is protonated versus unprotonated. These ambiguities illustrate that there are still many questions that need to be answered concerning the stability of amino-substituted acridines and the mechanisms of hydrolysis.

There have been several computational studies published on acridines in general.[6−9] Existing work in the area of quantum chemical properties of acridines mainly consists of photophysical properties such as absorption and emission.[6] For example, Oliveira and co-workers have investigated the differences in absorption/emission properties between neutral and protonated acridine-9-*N*-methacrylamides.[7] Their work also utilized bond order calculations to quantify the delocalization of a positive charge after protonation. Another study investigated the basicity of 9-substituted acridine-4-carboxamides.[8] An X-ray structural analysis and quantum chemistry study revealed that the dimethylamino group in 9-dimethylaminoacridine is twisted out from the plane of the acridine moiety as a result of steric effects.[9] To the best of our knowledge, there has not been a publication involving a computational investigation on the stability of acridines to hydrolysis.

In this study, we investigate the pH-dependent hydrolysis rates for 9-amino-substituted acridines using a combination of experimental and computational techniques. To gain insight into the forces that drive hydrolysis, ab initio quantum mechanics calculations are performed and applied to examine the physical properties of the C^9-N^{15} scissile bond. An analysis of the bond orders, bond dissociation energies, and rotational barriers is presented and applied to explain differences in the experimental rates of hydrolysis. Structural models are also evaluated to gain insight into the effect steric interactions have on the nature of the C^9-N^{15} bond as well as the experimental trends observed for hydrolysis.

MATERIAL AND METHODS

Synthesis. The synthesis of acridines **8a**−**f** (see Figure 2) began with a modified Ullmann−Goldberg coupling between 4-aminobenzoic acid (**4**) and 2-chlorobenzoic acid (**5**), which yielded the *N*-phenylanthranilic acid (**6**) as shown in Scheme 1.[10,11] This reaction requires copper(0) as a catalyst. Cocatalyst copper(I) iodide and pyridine are responsible for maintaining the catalytic cycle of copper(0), which reduces the reaction time and increases yields. Cyclization in refluxing $POCl_3$ afforded the 9-chloroacridine intermediate and produced an acid chloride of the second carboxylic acid.[1]

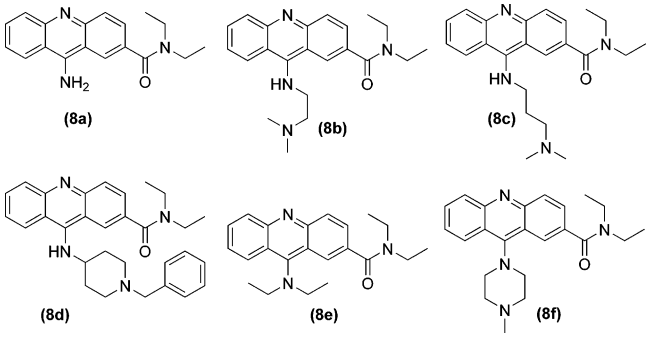

Figure 2. Compounds investigated in this study.

Subsequent reaction with diethylamine yielded the diethylamide-substituted 9-chloroacridine. Reaction with phenol with mild heating produced the key 9-phenoxyacridine intermediate (**7**). The final step entailed reacting the 9-phenoxy intermediate with the desired amine, resulting in the 2-diethylamide-substituted 9-aminoacridine (**8a**−**f**).[12] It should be noted that compound **8e** could not be synthesized in this manner and was, therefore, unavailable for hydrolysis experiments.

Hydrolysis Reaction. Hydrolysis reactions were performed in triplicate at 37 °C on a Bruker-7400 UV/vis spectrometer over a 6 h period. Table 1 shows the buffers, concentration, and pH for each reaction. MES, HEPES, and CHES buffers (commercial vendors) were chosen because they give an overall range of 5 pH units between 5.3 and 10.3. Although each of the compounds investigated in this study has a unique spectrum, it was observed that they all share noticeably similar characteristics in the visible range. All the compounds are yellow in aqueous solution regardless of pH. This is beneficial for running the hydrolysis reactions because the two products (acridone and amine) are nearly colorless. This allows for the monitoring of hydrolysis by observing absorbance at a single wavelength in the visible region. The wavelength of 434 λ was selected because of the occurrence of an absorbance maximum at this wavelength for the majority of the compounds. The concentration of the compounds was approximately 67 μg/mL for all of the hydrolysis reactions. Because of a lack of solubility of the compounds in alkaline conditions, a concentration of 20% dimethyl sulfoxide (DMSO) was required. It was determined that the addition of DMSO had an insignificant effect on the hydrolysis rate. The hydrolysis rates were calculated from the spectroscopy data by nonlinear curve fitting using a single-exponential decay function in the Origin 7.5 program (Originlab, Northhampton, MA). The results are reported as $t_{1/2}$ values. In cases where substantial decay during the time frame of the experiment could not be observed and accurate predictions are not feasible, hydrolysis rates were arbitrarily assigned to be larger than 144 h. Thus, compounds with a $t_{1/2}$ greater than 144 h can be considered stable under these conditions.

Determination of Energy of Activation. The energies of activation for the hydrolysis reaction were determined experimentally by investigating the temperature dependence on the hydrolysis rate. For compound **8d**, the rate constants for hydrolysis were determined at pH 7.3 and 9.3 in the range from 30 to 70 °C. The same experimental procedure for determining hydrolysis rates was used with the exception of an 8 h time period. The rate constants (k) were calculated

Scheme 1. Synthetic Pathway for 9-Aminoacridines[a]

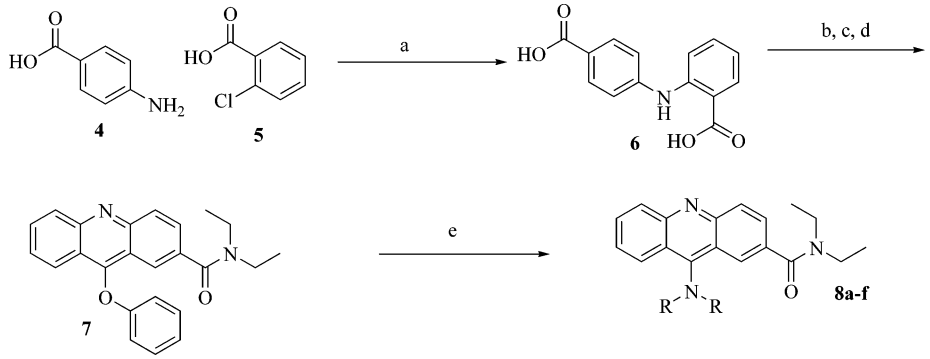

[a] Reagents and conditions: (a) Cu, CuI, pyridine, K_2CO_3, H_2O, reflux; (b) $POCl_3$, reflux; (c) *N*,*N*-diethylamine, CH_2Cl_2, 0 °C; (d) phenol, 60 °C; (e) amine, 120 °C.

Table 1. Buffer Specifications for Hydrolysis Reactions

buffer	0.1 M MES		0.1 M HEPES		0.1 M CHES	
pH	5.30	6.30	7.30	8.30	9.30	10.30

from the $t_{1/2}$ values using the equation $k = \ln(2)/t_{1/2}$. The energy of activation was determined by nonlinear curve fitting in Origin 7.5 using the Arrhenius equation, $k = A\,e^{-E/RT}$, where k is the rate constant, A is a constant, E is the energy of activation, T is the temperature in K, and R is the gas constant. The constant A was assumed to be independent of temperature in the temperature range studied.

Determination of pK_a's. Experimental pK_a's were determined by titration using an Accumet XL15 pH meter. The dihydrochloride salts of compounds **8b** and **8c** dissolved in 50% DMSO were titrated with 0.1 N NaOH. All titrations were conducted in triplicate at room temperature. The pK_a values were computed from the first derivative of the titration curves using a peak-fitting function with Gaussian line shapes in Origin 7.5.

Computational. Ab initio quantum chemical calculations were conducted using the Gaussian 03 suite of programs.[13] Since we were interested in the delocalization of electrons, a theory level which incorporates electron correlation was used. Essentially, this meant that Møller−Plesset perturbation theory (MP2 or greater) or a density function theory (DFT) method was required. Because of the high computational demands of MP2 level calculations, the much more economical DFT level of theory was preferred. In this study, the third generation hybrid DFT B1B95, which includes kinetic energy properties, was applied.[14] The B1B95 method has been proven to have excellent performance on energy calculations and better performance than B3LYP on thermochemical kinetics.[15,16] Structures were initially optimized at the HF/3-21g* theory level and subsequently optimized with the hybrid DFT B1B95 with a 6-31+g** basis set. The basis set of 6-31+g** was selected for all subsequent calculations. Test calculations indicated that higher basis sets such as 6-311g** and 6-311+g** did not provide a significant improvement and, therefore, were not used. Normal mode calculations were conducted on the final optimized structures to verify that the final structures were in fact minima by examination of the vibrational frequencies. The calculations were also repeated using a continuum solvation model. The method of choice was the C-PCM, conductor-like polarizable continuum model, using water as a solvent, as implemented in Gaussian 03.[17]

The bond orders were calculated from the DFT-optimized structures using the natural bond orbital (NBO) function in Gaussian 03. The bond dissociation energies were derived by homolytic cleavage of the C^9-N^{15} bond and subsequent optimization of the fragments using UB1B95. The bond dissociation ΔE was calculated from single-point energies of the optimized starting structure and resulting fragments using the equation $\Delta E = E_{\text{products}} - E_{\text{reactants}}$. The rotational energies were estimated for the C^9-N^{15} bond using the equation $\Delta E = E(90°) - E(0°)$. Optimizations fixing the C^9-N^{15} bond dihedral at 0° and 90° (when necessary) were performed. The importance of these torsions was determined from potential energy scans and geometric inspections of maxima and minima conformations. In the case of the neutral molecules, the exocyclic nitrogen has a pyramidal configuration requiring the dihedrals to be slightly greater or less than 0° and 90°. This was done to ensure that the nitrogen was in fact coplanar or perpendicular, respectively. These two dihedrals were deemed to be particularly important because they represent maximal or minimal delocalization potential across the C^9-N^{15} bond. All single-point energies were calculated utilizing SCF=tight. Bond lengths and torsional angles were extracted from optimized structures. Calculations were conducted on both the unprotonated and protonated N^{10} species. To be able to perform the DFT calculations in a reasonable time frame, the molecular structures of compounds **8a**−**f** were simplified. The two ethyl portions of the diethylamide substitution and the phenyl ring of compound **8d** were not included.

RESULTS AND DISCUSSION

Hydrolysis Reaction. A summary of the rates of hydrolysis in MES, HEPES, and CHES is given in Table 2. The results show that compound **8a** (the only primary amine in this study) has the slowest rate of hydrolysis over the entire pH range investigated here. Therefore, having essentially no steric interactions, compound **8a** is considered stable under all of the investigated hydrolysis conditions.

In the case of compounds **8b** and **8c** (both secondary amines), a substantially different result is seen as compared to that of compound **8a**. Compound **8b** undergoes significant hydrolysis under all reaction conditions examined, exhibiting the shortest $t_{1/2}$ times between the pHs of 6.30 and 9.30. A plot of the $t_{1/2}$ versus pH overlaid on a first derivative titration plot, as shown in Figure 3a, shows that hydrolysis is fastest between the pK_a's for the distal dimethyl tertiary amine and

Table 2. Results from Hydrolysis Reactions Reported as Calculated $t_{1/2}$ Measured in Hours

	0.1 M MES pH		0.1 M HEPES pH		0.1 M CHES pH	
compound	5.30	6.30	7.30	8.30	9.30	10.30
8a	≫144	≫144	≫144	≫144	>144	>144
8b	23.12 ± 0.47	7.50 ± 0.04	2.62 ± 0.02	2.36 ± 0.02	5.30 ± 0.03	17.27 ± 0.13
8c	≫144	>144	31.57 ± 0.88	10.33 ± 0.15	11.12 ± 0.12	29.02 ± 0.44
8d	>144	>144	>144	107.07 ± 10.40	83.19 ± 2.40	115.60 ± 3.36
8e						
8f	0.44 ± 0.03	1.32 ± 0.04	3.27 ± 0.01	8.27 ± 0.04	25.33 ± 0.61	39.41 ± 2.17

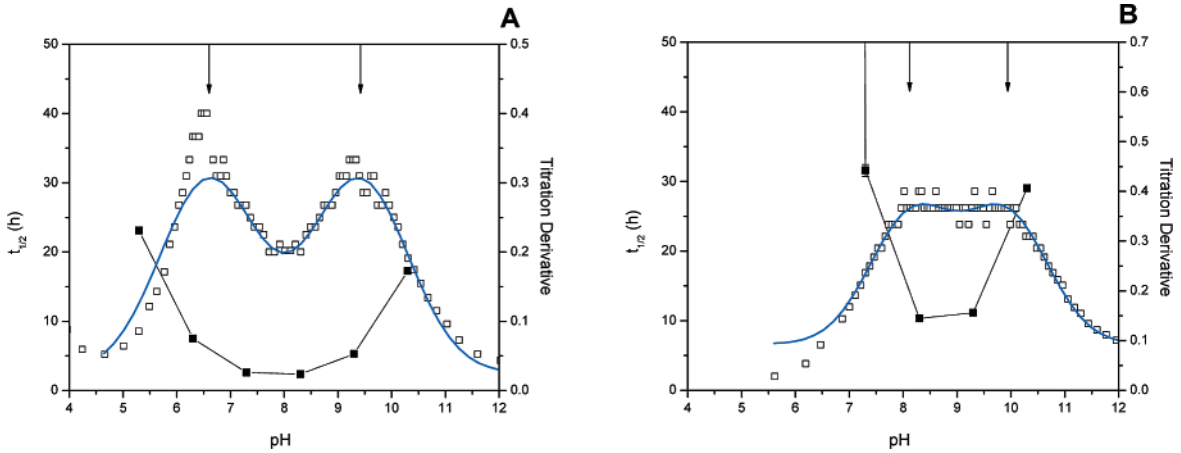

Figure 3. $t_{1/2}$ versus pH (filled squares) and titration derivative versus pH (open squares), solid lines represent fitted peaks, for compound **8b** (A) and **8c** (B). The arrows at the top represent the determined pK_a points of 6.6 and 9.4 for compound **8b** and 8.1 and 9.9 for compound **8c**.

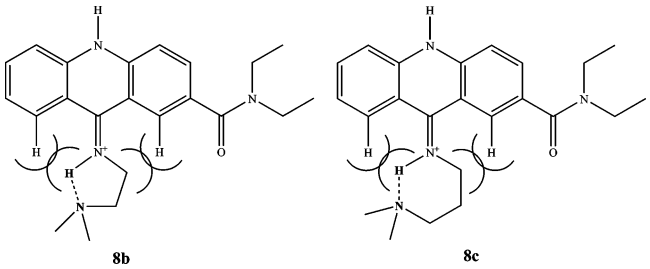

Figure 4. Structures illustrating the proposed intramolecular hydrogen bond in compounds **8b** and **8c**, as indicated by a dotted line.

the acridine vinylogous amidine. Experimentally determined pK_a's were estimated to be 6.6 and 9.4 for compound **8b**. Similarly, compound **8c** hydrolyzes fastest between pH 8.3 and 9.3, which corresponds well with the experimentally determined pK_a's of 8.1 and 9.9 as shown in Figure 3b.

When compounds **8b** and **8c** are under acidic conditions, both the distal dimethyl tertiary amine and the acridine vinylogous amidine carry a positive formal charge, leading to charge−charge repulsion. Recall that protonation occurs at the N^{10} position and the resulting positive charge is delocalized through resonance with the exocyclic nitrogen on the 9 position (proximal nitrogen). This charge repulsion favors an extended conformation. At a pH between the two pK_a's for compounds **8b** and **8c,** the distal nitrogen carries no charge. This allows the distal nitrogens to form internal hydrogen bonds, forming a five- or six-member ring, respectively, as shown in Figure 4. These pseudo tertiary amines may act to accelerate hydrolysis by adding steric bulk or by facilitating hydrolysis through anchimeric assistance. The term "anchimeric assistance" pertains to the acceleration of a reaction by intramolecular participation of functional groups, resulting in catalysis of the reaction.[18,19] When the pH is above both the pK_a's for compounds **8b** and **8c**, the molecules are neutral and, presumably, hydrolysis proceeds without acceleration.

Compound **8d** (another secondary amine) is substantially more stable than either **8b** or **8c**. Structurally, **8d** is a constrained analogue of **8c,** which prevents internal hydrogen bond formation. In addition, compound **8d** has increased steric mass located away from the acridine moiety, which does not result in steric interactions. However, this steric mass may partially prevent access of the hydroxide ions, thus increasing $t_{1/2}$ values. Overall, the hydrolysis of secondary amines appears to be favored under alkaline conditions, as exemplified by compound **8d**. To understand the energetics behind faster hydrolysis under alkaline conditions, we studied the temperature dependence on the hydrolysis rate. The temperature-dependence study allows for the determination of the energy of activation. The energies of activation for compound **8d** were determined to be 19.93 kcal/mol at pH 7.3 and 19.51 kcal/mol at pH 9.3, resulting in a 0.4 kcal/mol lower energy of activation under alkaline conditions.

In contrast, compound **8f** (a tertiary amine) demonstrates faster rates of hydrolysis under acidic conditions rather than alkaline. However, the results also indicate that significant levels of hydrolysis occur under alkaline conditions. As previously mentioned, Ledóchowski and co-workers proposed that hydrolysis is favored under alkaline conditions involving the attack of a hydroxide ion. Under acidic conditions, hydroxide ion concentrations are extremely low, and therefore, hydrolysis could be proceeding through a Schiff bases mechanism. As was discussed earlier, protonation of the N^{10} position of 9-aminoacridines, followed by delocalization of the positive charge, results in an increase in double-bond character between the C^9-N^{15} positions, as shown in Figure 5. The resonance form in which a double

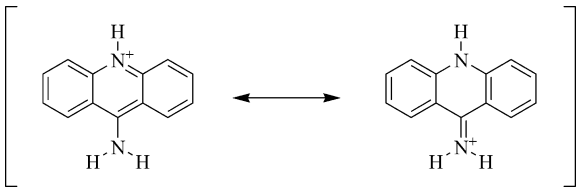

Figure 5. Resonance forms of the protonated 9-aminoacridine.

bond exists between the C^9-N^{15} positions resembles that of a Schiff base, which can undergo hydrolysis via the attack by water.[20−22] Because of steric interactions, the resulting hemi-aminol intermediate readily loses the amine to form a ketone, as shown in Figure 2. Secondary amines have the same delocalization. However, since the steric interactions are significantly less, there is a general strengthening of the C^9-N^{15} bond, rather than a weakening due to steric interactions. Therefore, the results indicate that the existence of large amounts of steric bulk around the 9-amino position results in an increase of hydrolysis under acidic conditions.

Computational. Wiberg bond orders generated from the NBO calculations are reported in Tables 3 and 4. While focusing at the bond of interest, C^9-N^{15}, a definite correlation can be seen between neutral molecules versus molecules protonated at the N^{10} position. Each compound shows greater bond orders between C^9-N^{15} when the molecules are protonated, as is expected. Recall that this effect is due to the delocalization of the positive charge, as was previously discussed. The results for the neutral molecules show a clear trend. As steric bulk increases, from primary to secondary to tertiary amines, the bond orders decrease. This indicates that, under alkaline conditions, steric interactions are diminishing the potential for delocalization. When comparing the bond orders for the six compounds under acidic conditions (protonated N^{10}), there is no apparent trend. The results do not show an overriding decrease in bond order going from primary to secondary to tertiary substituted amines.

The only compound which demonstrated a decrease in bond order was compound **8f**, where the C^9-N^{15} bond rotates out of the plane by approximately 45°. For all other compounds investigated in this study, this angle optimizes close to 0°. To investigate the relevance of the 45° rotation in compound **8f**, a conformational constraint was imposed by fixing the torsional angle at 0°. Subsequent minimization resulted in a structure which is 1.33 kcal/mol higher in energy. Interestingly, NBO calculations performed on the constrained **8f** compound produced a bond order comparable with those of the other compounds in the series. An inspection of the optimized structure, shown in Figure 6b, shows the constrained molecule is severely distorted from planarity. This clearly demonstrates that steric strain is a driving force in reducing the bond order of the C^9-N^{15} bond, leading to faster rates of hydrolysis.

As shown in Tables 3 and 4, the results from bond dissociation energy calculations correlate well with the results from the NBO calculations. In comparing the gas-phase data from the neutral versus the protonated N^{10} molecules, it is apparent that protonated compounds have higher bond dissociation energies. Furthermore, clear trends are observed going from primary to secondary to tertiary substituted amines under both neutral and protonated N^{10} states. Once again, the results suggest that increasing the amounts of steric bulk weakens the C^9-N^{15} bond, leading to faster rates of hydrolysis. It is possible that results from gas-phase calculation may not accurately reflect experimental data on molecules in solution. To verify this, bond dissociation energies were calculated incorporating the C-PCM continuum solvation model. The results indicate that the energies are within the same range as gas-phase calculations. More importantly, the same trends are observed whether using gas-phase or solvated calculations. This suggests that solvation effects do not have a significant impact on the bond dissociation energy. This is not surprising as covalent bond energies are less

Table 3. Physical Properties for the Optimized Acridine Structures under Neutral Conditions

compound	C^9-N^{15} torsion[a]	C^9-N^{15} length (Å)	bond order C^9-N^{15}	bond dissociation (kcal/mol)	solvation bond dissociation (kcal/mol)	rotational energy[b] (kcal/mol)	solvation rotational energy[b] (kcal/mol)
8a	17.278	1.360	1.311	113.46	127.57	8.41	9.78
8b	18.960	1.356	1.232	98.51	105.93	3.97	4.21
8c	16.690	1.350	1.251	102.20	109.54	3.96	3.33
8d	23.485	1.358	1.224	99.74	108.16	2.11	3.31
8e	80.323	1.403	1.043	86.51	93.65	−6.56	−5.00
8f	72.335	1.418	0.992	86.46	92.83	−12.63	−10.00

[a] Torsional angle centered on C^9-N^{15} bond. [b] $\Delta E = E(90°) - E(0°)$.

Table 4. Physical Properties for the Optimized Acridine Structures under Acidic Conditions

compound	C^9-N^{15} torsion[a]	C^9-N^{15} length (Å)	bond order C^9-N^{15}	bond dissociation kcal/mol	solvation bond dissociation (kcal/mol)	rotational energy[b] (kcal/mol)	solvation rotational energy[b] (kcal/mol)
8a	0.682	1.328	1.506	126.39	139.40	13.08	13.49
8b	0.669	1.318	1.405	125.64	122.77	13.24	11.41
8c	10.641	1.317	1.432	123.20	121.66	9.81	7.29
8d	0.444	1.324	1.406	118.94	119.89	12.82	9.38
8e	3.905	1.323	1.461	102.39	103.85	7.29	5.28
8f (45)	44.773	1.348	1.287	103.10	103.76	7.57[c]	5.79[c]
8f (0)[d]	0.622	1.323	1.466	101.86	102.96	−1.33[e]	−0.80[e]

[a] Torsional angle centered on C^9-N^{15} bond using heavy atoms when possible. [b] $\Delta E = E(90°) - E(0°)$. [c] Energy difference determined by $E(90°) - E(45°)$. [d] Conformational constraint imposed. [e] Reference conformation is 45°.

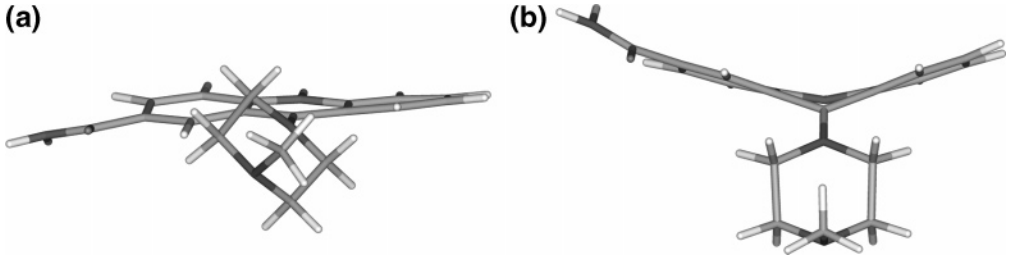

Figure 6. Structure of compound **8f** at global minima with an observed angle around the C^9-N^{15} bond at 45° (a, on the left) and an optimized structure of **8f** where the C^9-N^{15} angle has been fixed at 0° (b, on the right). Observe how steric clashes between the piperazine and the acridine cause a distortion of the acridine moiety.

susceptible to solvent effects as are their nonbonding counterparts such as salt links or hydrogen-bond interactions.

The results of the rotational energy calculations [$\Delta E = E(90°) - E(0°)$] are shown in Tables 3 and 4. Under acidic conditions, the primary and secondary amines show similar energy differences. In comparing the ΔEs under neutral and protonated conditions, it is clear that protonation of N^{10} greatly favors an sp^2 or coplanar geometry. This effect is more evident for the secondary amines, which show much greater ΔE differentials upon protonation. This disparity is most likely due to steric interactions of the secondary amines that compete with delocalization in determining the conformation of the C^9-N^{15} bond. Even more striking are the results for the two tertiary amine compounds **8e** and **8f**. When compounds **8e** and **8f** are in the neutral state, the relaxation of steric interactions is far more important than the delocalization across the C^9-N^{15} bond and the conformations prefer a nonplanar orientation. Under acidic conditions, this trend is somewhat reversed and the preference shifts toward planarity. The exception is compound **8f**, which prefers a torsional angle of 45°. In this case, the added constraint of the piperazine ring most likely forces the ring out of planarity. The N-alkyl substitutions of **8e**, on the other hand, are more flexible and can rotate to avoid the severe steric clashes noted in Figure 6. This may explain the stability of **8e** in the planar configuration compared to that of **8f** (which fails to optimize to an extrema at this same point in conformational space about the C^9-N^{15} bond). Nevertheless, the results show that both **8e** and **8f** have a lower $\Delta E(90° - 0°)$, indicating that steric interactions are an important factor in increasing the rates of hydrolysis and, in the case of **8f**, greatly reduce both the bond order and bond strength.

CONCLUSIONS

This study has examined the hydrolysis rates of several amino-substituted acridines using a combination of experimental and computational techniques. The results have revealed that two opposing forces affect the rate of hydrolysis: delocalization across the C^9-N^{15} bond and steric interactions between the N substituents and protons on the acridine heterocycle. In the absence of steric interactions, the charge delocalization is the dominant force stabilizing the C^9-N^{15} bond. This effect is further increased under acidic conditions as a result of N^{10} protonation which, in turn, increases the potential for delocalization. The results further show that, as steric interactions increase, bond orders and bond strengths decrease as the "cost" of rotating the C^9-N^{15} toward 0° increases. The most striking result is seen in the tertiary amine **8f**, which fails to reach planarity when optimized. Overall, the data nicely explains the trends in hydrolysis observed for the substituted acridines, suggesting that computational methods of this type may be useful in evaluating rates of bond cleavage in a greater variety of molecular systems. While a reaction coordinate calculation would provide a more detailed view and evaluation of the energies and structures effecting bond hydrolysis, such calculations are beyond the scope of this work. A preliminary evaluation of the potential steps and structures associated with a calculation of this type revealed that the system is significantly more complex than those reported in the literature.[23,24] Work is underway to define and evaluate several pathways under acidic, basic, and neutral conditions using a combination of quantum mechanical (QM) and molecular mechanical (MM) methods, and such studies will be the topic of a future report.

In reviewing the results, the decreased stability of compounds **8b** and **8c** are admittedly the most unexpected. Considering that both compounds **8b** and **8c** are secondary amines, we anticipated that these compounds would be as stable as the similar secondary amine **8d**. In fact, bond orders and bond energies for these three compounds also suggest that they should have similar stabilities. An evaluation of the pK_a's and pH-dependent rates for these compounds, however, led to the development of a structural model that explains the apparent disparities in hydrolysis rates on the basis of the formation of a five- or six-membered intramolecular hydrogen bond. Such interactions are not unprecedented. Acceleration of chemical reactions involving anchimeric effects have been widely studied in physical organic chemistry.[18,19] More recently, evidence has suggested that an acceleration of substrate hydrolysis exists in biological systems including GTPases, serine proteinases, and glycosidases.[19,25,26] Although the majority of the anchimeric assistance examples involve covalent linkages, we feel that the internal hydrogen bond significantly polarizes the C^9-N^{15} bond, greatly accelerating the rate of hydrolysis. Alternatively, or in conjunction, intramolecular ring formation may increase steric interactions, further accelerating hydrolysis.

Finally, the results can be applied to shed insight into the probable mechanism of hydrolysis for the compounds studied here. The results generally support the hydroxide displacement mechanism proposed by Ledóchowski and co-workers for substituted acridines. This mechanism involves the attack of C^9 by a hydroxide ion, leading to bond cleavage and subsequent formation of the acridone moiety. The exception is **8f**, which shows faster rates of hydrolysis under acidic conditions. The results presented here indicate this may be due to the induction of severe steric strain under acidic

conditions, which greatly weakens the C^9-N^{15} bond. In this case, hydrolysis would proceed by the attack of water similar to the acid-catalyzed hydrolysis mechanism of Schiff bases. It could also be argued that, under alkaline conditions, the piperazine ring is rotated out of the plane of the acridine rings, effectively blocking attack by the hydroxide ion. Taken overall, the results suggest that more than one mechanism may exist for the hydrolysis of substituted acridines. Progress in developing the correct reaction coordinates and pathways using theoretical techniques may go a long way in understanding these mechanisms and differences in rates of hydrolysis. Calculations of this type, however, represent some of the most challenging problems facing computational chemists today. While great progress has been made in developing QM/MM methods that can handle reaction coordinates in solution (and in proteins), such methods are still limited by our understanding of the mechanism and structures that populate the reaction pathway. Given the complexity of most interesting chemical reactions, it is fair to say that we have only begun to scrape the edge of complexity for problems of this type.

EXPERIMENTAL SECTION

*N-(4-Carboxyphenyl)anthranilic Acid (**6**).* Potassium carbonate (30.6 mmol) was first dissolved in 100 mL of distilled water. Next, 2-chlorobenzoic acid (**5**; 20.4 mmol) was added, followed by 4-aminobenzoic acid (**4**; 40.8 mmol), pyridine (0.3 mL), copper(0) (0.1 g), and copper(I) iodide (0.1 g). The reaction was stirred under reflux for 4 h. Once the reaction was cooled, just enough 5% NaOH(aq) was added to completely dissolve the product. The mixture was then passed through a fritted filter containing a thin layer of silica gel between two layers of compressed Celite and was rinsed with saturated $NaHCO_3$ to remove the copper catalyst. The resulting filtrate was acidified using 3 M HCl(aq) until the pH equaled 1. The resultant yellow precipitate (2-phenylamino-terephthalic acid) was then filtered and recrystallized from absolute ethanol/water. Yield ~ 43.1%. ^{1}H NMR (300 MHz, DMSO-d_6): δ 6.92 (m, 1H), 7.26 (d, 2H), 7.48 (m, 2H), 7.85 (d, 2H), 7.93 (d, 1H), 9.79 (s, 1H).

*N,N-Diethyl-9-phenoxyacridine-2-carboxamide (**7**).* *N*-(4-Carboxyphenyl)anthranilic acid (**6**; 7.77 mmol) was dissolved in $POCl_3$ (~50 mL) and refluxed for 1 h. Excess $POCl_3$ was then recovered via vacuum distillation being careful not to heat the reaction flask over 100 °C. The resulting residue was then dissolved in CH_2Cl_2 (~50 mL) and cooled to 0 °C in an ice bath. Then, an excess amount of diethylamine (~4 mL) was added dropwise while stirring. The reaction was allowed to warm to room temperature and was slightly heated while stirring for approximately 1 h. Then, the reaction was condensed and left in a vacuum to remove residual amounts of amine. After 2 days on the pump, phenol (~15 g) was added to the reaction flask and heated to 80 °C for 30 min with manual stirring using a thermometer. The reaction was then cooled and diluted with 200 mL of CH_2Cl_2. The mixture was then washed with 30% w/w NaOH in water (150 mL × 2) to remove phenol, washed with brine (150 mL), dried over $MgSO_4$, and concentrated. Thin-layer chromatography showed multiple spots, but the product is the major spot, as seen by elution with 15:1 CH_2Cl_2/MeOH. The product was purified by silica chromatography eluting with 15:1 CH_2Cl_2/MeOH. Fractions containing the product were combined and concentrated. The resulting solid was dissolved in minimal amounts of EtOAc and precipitated out with petroleum ether or hexanes, yielding the desired product. Yield = 42.7%. ^{1}H NMR (300 MHz, $CDCl_3$): δ 0.96 (s br, 3H), 1.24 (s br, 3H), 3.21 (s br, 2H), 3.53 (s br, 2H), 6.85 (d, 2H), 7.06 (t, 1H), 7.28 (m, 2H), 7.50 (m, 1H), 7.83 (m, 2H), 8.12 (m, 2H), 8.29 (t, 2H).

*General Procedure for 9-Amino-acridine-2-carboxamides (**8a**−**f**).* 9-phenoxy-acridine-2-carboxamide (5 mmol) was dissolved in 2 mL of amine (for example, 4-amino-*N*-benzylpiperidine) and heated to 120 °C for 15 min. The reaction was cooled and run on a silica column to purify the product and remove excess amine. A solvent ratio of 15:1 CH_2Cl_2/MeOH was used for the first 200 mL followed by 15:1:0.1 CH_2Cl_2/MeOH/NEt_3 until the product eluted from the column. The fractions with the product were collected and concentrated. The yellow product was dissolved in EtOAc and precipitated out with petroleum ether or hexanes, yielding the 9-amino-acridine-2-carboxamide.

*9-Amino-N,N-diethylacridine-2-carboxamide (**8a**).* Yield = 72.4%. ^{1}H NMR (300 MHz, $CDCl_3$): δ 1.24 (s br, 6H), 3.38 (s br, 2H), 3.59 (s br, 2H), 5.70 (s br, 2H), 7.43 (t, 1H), 7.66 (d, 1H), 7.73 (t, 1H), 7.91 (d, 1H), 8.08 (m, 3H). HRMS ($C_{18}H_{20}N_3O$) *m*/*z*: $[M+H]^+$ found, 294.1588; calcd, 294.1601.

*9-(2-(Dimethylamino)ethylamino)-N,N-diethylacridine-2-carboxamide (**8b**).* Yield = 51.2%. ^{1}H NMR (300 MHz, $CDCl_3$): δ 1.24 (s br, 6H), 2.37 (s, 3H), 2.62 (t, 2H), 3.49 (s br, 4H), 3.91 (t, 2H), 7.38 (t, 1H), 7.64 (d, 1H), 7.69 (t, 1H), 8.064 (d, 1H), 8.07 (d, 1H), 8.17 (d, 1H), 8.27 (s, 1H). HRMS ($C_{22}H_{29}N_4O$) *m*/*z*: $[M+H]^+$ found, 365.2307; calcd, 365.2336.

*9-(3-(Dimethylamino)propylamino)-N,N-diethylacridine-2-carboxamide (**8c**).* Yield = 55.3%. ^{1}H NMR (300 MHz, $CDCl_3$): δ 1.22 (s br, 6H), 1.89 (t, 2H), 2.42 (s, 6H), 2.68 (t, 2H), 3.48 (s br, 4H), 4.14 (t, 2H), 7.27 (t, 1H), 7.58 (d, 1H), 7.641 (t, 1H), 7.95 (d, 1H), 8.02 (d, 1H), 8.13 (d, 1H), 8.23 (s, 1H). HRMS ($C_{23}H_{31}N_4O$) *m*/*z*: $[M+H]^+$ found, 379.2471; calcd, 379.2492.

*9-(1-Benzylpiperidin-4-ylamino)-N,N-diethylacridine-2-carboxamide (**8d**).* Yield = 50.7%. ^{1}H NMR (600 MHz, $CDCl_3$): δ 1.23 (s br, 6H), 1.75 (m br, 2H), 2.07 (m br, 4H), 2.87 (m br, 2H), 3.41 (s br, 2H), 3.51 (s, 2H), 3.63 (s br, 2H), 3.88 (s br, 1H), 4.76 (s br, 1H), 7.26 (m, 1H), 7.30 (m, 4H), 7.44 (t, 1H), 7.68 (d, 1H), 7.74 (t, 1H), 8.07 (d, 1H), 8.12 (m, 2H), 8.22 (s, 1H). HRMS ($C_{30}H_{35}N_4O$) *m*/*z*: $[M+H]^+$ found, 467.2776; calcd, 467.2805.

*9-(Diethylamino)-N,N-diethylacridine-2-carboxamide (**8e**).* Not able to synthesize.

*N,N-Diethyl-9-(4-methylpiperazin-1-yl)acridine-2-carboxamide (**8f**).* Yield = 43.1%. ^{1}H NMR (300 MHz, DMSO-d_6): δ 1.18 (s br, 6H), 2.33 (s, 3H), 2.64 (t, 4H), 3.36 (s br, 4H), 3.61 (t, 4H), 7.56 (t, 1H), 7.70 (d, 1H), 7.79 (t, 1H), 8.09 (d, 1H), 8.10 (d, 1H), 8.25 (s, 1H), 8.37 (d, 1H). HRMS ($C_{23}H_{29}N_4O$) *m*/*z*: $[M+H]^+$ found, 377.2310; calcd, 377.2336.

REFERENCES AND NOTES

(1) Albert, A. *The Acridines: Their Preparation, Physical, Chemical, and Biological Properties and Uses*, 2nd ed.; Edward Arnold Ltd.: London, 1966.

(2) Chiron, J.; Galy, J. Reactivity of the acridine ring: a review. *Synthesis* **2004**, *3*, 313−325.

(3) Wainwright, M. Acridine-a neglected antibacterial chromophore. *J. Antimicrob. Chemother.* **2001**, *47*, 1−13.
(4) Denny, W. A. Acridine derivatives as chemotherapeutic agents. *Curr. Medicinal Chem.* **2002**, *9*, 1655−1665.
(5) Ledóchowski, A.; Sobczyk, Z.; Kunikowski, A.; Kowalewska, G. Reactions at C^9 of acridine derivatives. Part XIII. Hydrolysis of derivatives of 9-aminoacridine. *Rocz. Chem.* **1976**, *50*, 1267−1272.
(6) Rubio-Pons, O.; Serrano-Andrés, L.; Merchán, M. A Theoretical Insight into the Photophysics of Acridine. *J. Phys. Chem. A.* **2001**, *105*, 9664−9673.
(7) Oliveira, H. P. M.; Camargo, A. J.; de Macedo, L. G. M.; Gehlen, M. H.; da Silva, A. B. F. A quantum chemical and photophysical study of acridine-9-N-methacrylamide. *THEOCHEM* **2004**, *674*, 213−225.
(8) Parajuli, R.; Medhi, C. Basicities of some 9-substituted acridine-4-carboxamides: A density functional theory (DFT) calculation. *J. Chem. Sci.* **2004**, *116*, 235−241.
(9) Rak, J.; Krzymiński, K.; Skurski, P.; Jóźwiak, L.; Konitz, A.; Dokurno, P.; Błażejowski, J. X-ray, Quantum Mechanics and Density Functional Methods in the Examination of Structure and Tautomerism of *N*-Methyl-Substituted Acridin-9-amine Derivatives. *Aust. J. Chem.* **1998**, *51*, 643−651.
(10) Pellón, R. F.; Carrasco, R.; Rodés, L. Synthesis of N-phenylanthranilic acids using water as solvent. *Synth. Commun.* **1993**, *23* (10), 1447−1453.
(11) Pellón, R. F.; Carrasco, R.; Millian, V.; Rodés, L. Use of pyridine as cocatalyst for the synthesis of 2-carboxy diphenyl ethers by Ullmann−Goldberg condensation. *Synth. Commun.* **1995**, *25* (7), 1077−1083.
(12) Rewcastle, G. W.; Atwell, G. J.; Chambers, D.; Baguley, B. C.; Denny, W. A. Potential antitumor agents. 46. Structure−activity relationships for scridine monosubstituted derivatives of the antitumor agent N-[2-(dimethylamino)ethyl]-9-amino-4-carboxamide. *J. Med. Chem.* **1986**, *29*, 472−477.
(13) Frisch, M. J.; Trucks, G. W.; Schlegel, H. B.; Scuseria, G. E.; Robb, M. A.; Cheeseman, J. R.; Montgomery, J. A., Jr.; Vreven, T.; Kudin, K. N.; Burant, J. C.; Millam, J. M.; Iyengar, S. S.; Tomasi, J.; Barone, V.; Mennucci, B.; Cossi, M.; Scalmani, G.; Rega, N.; Petersson, G. A.; Nakatsuji, H.; Hada, M.; Ehara, M.; Toyota, K.; Fukuda, R.; Hasegawa, J.; Ishida, M.; Nakajima, T.; Honda, Y.; Kitao, O.; Nakai, H.; Klene, M.; Li, X.; Knox, J. E.; Hratchian, H. P.; Cross, J. B.; Bakken, V.; Adamo, C.; Jaramillo, J.; Gomperts, R.; Stratmann, R. E.; Yazyev, O.; Austin, A. J.; Cammi, R.; Pomelli, C.; Ochterski, J. W.; Ayala, P. Y.; Morokuma, K.; Voth, G. A.; Salvador, P.; Dannenberg, J. J.; Zakrzewski, V. G.; Dapprich, S.; Daniels, A. D.; Strain, M. C.; Farkas, O.; Malick, D. K.; Rabuck, A. D.; Raghavachari, K.; Foresman, J. B.; Ortiz, J. V.; Cui, Q.; Baboul, A. G.; Clifford, S.; Cioslowski, J.; Stefanov, B. B.; Liu, G.; Liashenko, A.; Piskorz, P.; Komaromi, I.; Martin, R. L.; Fox, D. J.; Keith, T.; Al-Laham, M. A.; Peng, C. Y.; Nanayakkara, A.; Challacombe, M.; Gill, P. M. W.; Johnson, B.; Chen, W.; Wong, M. W.; Gonzalez, C.; Pople, J. A. *Gaussian 03*, revision C.01; Gaussian, Inc.: Wallingford, CT, 2004.
(14) Becke, A. D. Density-functional thermochemistry. IV. A new dynamical correlation functional and implications for exact-exchange mixing. *J. Chem. Phys.* **1996**, *104*, 1040−1047.
(15) Zhao, Y.; Pu, J.; Lynch, B. J.; Truhlar, D. G. Tests of second-generation and third-generation density functionals for thermochemical kinetics. *Phys. Chem. Chem. Phys.* **2004**, *6*, 673−676.
(16) Zhao, Y.; Lynch, B. J.; Truhlar, D. G. Development and assessment of a new hybrid density functional model for thermochemical kinetics. *J. Phys. Chem. A* **2004**, *108*, 2715−2719.
(17) Cossi, M.; Rega, N.; Scalmani, G.; Barone, V. Energies, structures, and electronic properties of molecules in solution with the C−PCM solvation model. *J. Comput. Chem.* **2003**, *24*, 669−681.
(18) Jencks, W. *Catalysis in Chemistry and Enzymology*; McGraw-Hill, Inc: New York, 1969.
(19) Mark, B. L.; James, M. N. G. Anchimeric assistance in hexosaminidases. *Can. J. Chem.* **2002**, *80*, 1064−1074.
(20) Reeves, R. L. Schiff bases. Kinetics of hydrolysis of p-trimethylammoniumbenzylidene-p′-hydroxyaniline chloride in aqueous solution. *J. Am. Chem. Soc.* **1962**, *84*, 3332−3337.
(21) Sayer, J. M.; Conlon, P. The timing of the proton-transfer process in carbonyl additions and related reactions. General-acid-catalyzed hydrolysis of imines and N-acylimines of benzophenone. *J. Am. Chem. Soc.* **1980**, *102* (10), 3592−3600.
(22) Cordes, E. H.; Jencks, W. P. The mechanism of hydrolysis of Schiff bases derived from aliphatic amines. *J. Am. Chem. Soc.* **1963**, *85*, 2843−2848.
(23) Gorb, L.; Asensio, A.; Tunon, I.; Ruiz-Lopez, M. F. The mechanism of formamide hydrolysis in water from ab initio calculations and simulations. *Chem.—Eur. J.* **2005**, *11*, 6743−53.
(24) Lensink, M. F.; Mavri, J.; Berendsen, H. J. C. Simulation of slow reaction with quantum character: neutral hydrolysis of carboxylic ester. *J. Comput. Chem.* **1999**, *20*, 886−95.
(25) Fersht, A. Structure and mechanism in protein science: a guide to enzyme catalysis and protein folding; W. H. Freeman Publishing: New York, 1998.
(26) Dall′acqua, W.; Carter, P. Substrate-assisted catalysis: molecular basis and biological significance. *Protein Sci.* **2000**, *9*, 1−9.

CI050322S